Electronic energy-band structure of the $KMgF_3$ crystal

Richard A. Heaton and Chun C. Lin
Department of Physics, University of Wisconsin, Madison, Wisconsin 53706
(Received 10 March 1981; revised manuscript received 19 October 1981)

Electronic energy-band calculations have been performed for the $KMgF_3$ crystal by using the method of linear combinations of atomic orbitals with a self-consistent-field procedure. The basis set consists of 124 Bloch sums formed by atomic wave functions and single Gaussians. The wave functions of the valence-band states are composed mainly of F $2p$ orbitals. The bottom of the conduction band is an s-like (Γ_1) state. Slightly above this state are the K $3d$ bands which have sharp density of states. Transitions from the valence bands to these K $3d$ bands are responsible for the prominent features of the joint density of states below 20 eV and account for some of the structures in the measured optical dielectric function. Using $\alpha=1$ for the exchange parameter, we obtain a band gap of 9.6 eV, which is about 3 eV lower than the experimental value, but the calculated joint density of states involving the K $3d$ states show good agreement with optical measurements. By either raising α to 1.33 or using the $X\alpha\beta$ method we obtain a band gap of 12.4 eV, but the agreement between the joint density of states and optical data is worsened. Also the valence band becomes slightly narrower but its general features are unaltered. The band gap reduces to about 7 eV when we set α to $\frac{2}{3}$ or use the interpolation formula in the exchange approximation. The x-ray structure factors are calculated using five versions of the exchange approximation and the results all differ significantly from the experimental values.

I. INTRODUCTION

Crystals of the perovskite structure comprise a wide variety of properties. These include ferroelectric crystals ($BaTiO_3$), antiferromagnets ($KNiF_3$, $KMnF_3$), and nonmagnetic insulators ($KMgF_3$). Because of the relatively large number of atoms in a unit cell, first-principles calculations of the energy-band structure have been performed for only a few cases,[1,2] and no self-consistent-field (SCF) calculations, to our knowledge, have been reported. In this paper we present an SCF energy-band study for $KMgF_3$ which is one of the simplest perovskite crystals in that it is highly ionic, nonmagnetic, and has a simple cubic structure. The electronic states of the crystal are analyzed in terms of those of the constituent atoms, and the results are compared with optical experiments. Aside from the interest in the pure crystal, much attention has been given to point defects in $KMgF_3$ in recent years. A quantitative description of charge distribution in the pure crystal is needed for studying the electronic structure of point defects.

II. ENERGY-BAND CALCULATION

The crystal structure of $KMgF_3$ is of simple cubic (sc) type as shown in Fig. 1(a). Each unit cube contains an Mg atom at the center, a K atom at each corner, and an F atom at each face center; hence, one Mg, one K and three F atoms per unit cell. The lattice constant is $a=3.973$ Å. For linear combination of atom orbitals (LCAO) band calculations, we construct Bloch-sum basis functions for the Mg atoms, for the three sets of F atoms that are not translation-related to one another, and for the K atoms. If we place the origin at a Mg atom, these Bloch sums can be written as

$$b_i^{\mathrm{Mg}}(\vec{k},\vec{r})=\sum_\nu \exp(i\vec{k}\cdot\vec{R}_\nu)\phi_i^{\mathrm{Mg}}(\vec{r}-\vec{R}_\nu)\ ,$$

$$b_j^{\mathrm{F1}}(\vec{k},\vec{r})=\sum_\nu \exp(i\vec{k}\cdot\vec{R}_\nu)\phi_j^{\mathrm{F}}(\vec{r}-\vec{R}_\nu-\vec{t}_1)\ ,$$

$$b_j^{\mathrm{F2}}(\vec{k},\vec{r})=\sum_\nu \exp(i\vec{k}\cdot\vec{R}_\nu)\phi_j^{\mathrm{F}}(\vec{r}-\vec{R}_\nu-\vec{t}_2)\ , \quad (1)$$

$$b_j^{\mathrm{F3}}(\vec{k},\vec{r})=\sum_\nu \exp(i\vec{k}\cdot\vec{R}_\nu)\phi_j^{\mathrm{F}}(\vec{r}-\vec{R}_\nu-\vec{t}_3)\ ,$$

$$b_l^{\mathrm{K}}(\vec{k},\vec{r})=\sum_\nu \exp(i\vec{k}\cdot\vec{R}_\nu)\phi_l^{\mathrm{K}}(\vec{r}-\vec{R}_\nu-\vec{t}')\ ,$$

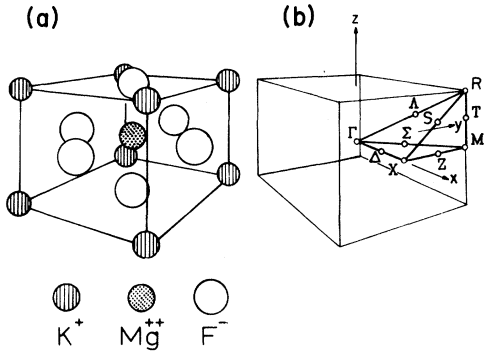

FIG. 1. (a) Crystal structure of $KMgF_3$. (b) Brillouin zone for the simple cubic lattice.

where $\vec{R}_\nu$ represents a translational vector for the sc lattice, and $\vec{t}$ and $\vec{t}\,'$ are vectors drawn from the origin to the F and K atoms, respectively, i.e.,

$$\begin{aligned}\vec{t}_1&=\tfrac{1}{2}a(1,0,0)\,,\\ \vec{t}_2&=\tfrac{1}{2}a(0,1,0)\,,\\ \vec{t}_3&=\tfrac{1}{2}a(0,0,1)\,,\\ \vec{t}\,'&=\tfrac{1}{2}a(1,1,1)\,.\end{aligned}\tag{2}$$

For a minimal basis set,[3,4] the localized functions ϕ are taken as the wave functions of all the occupied shells of the free ions, and for ease in computation, these atomic wave functions are expanded in terms of Gaussian-type orbitals (GTO), e.g.,

$$\phi_{ns}=\sum_i a_i\exp(-\beta_i r^2)\,,\tag{3}$$

etc. Furthermore, one can greatly reduce the computational work by using the same set of β's for all three kinds of atoms. A common Gaussian set is judiciously selected from the optimized exponents for K, Mg, and F given in the papers of Huzinaga[5] and Wachters,[6] by demanding that it accurately reproduce the free-ion SCF Hartree-Fock-Slater wave functions and energies.[7] The resulting β's are: 25 873, 5984.9, 1712.02, 563.304, 204.797, 80.4187, 51.4089, 33.1145, 19.9361, 9.862 21, 3.977 75, 2.691 63, 1.731 93, 0.977 055, 0.620 640, 0.396 147, 0.206 990, and 0.10, and they yield energy levels for K^+, Mg^{2+}, and F^- within 0.1% of the results of numerical solution of the Hartree-Fock-Slater equations. To test the wave functions we compute the free-ion atomic form factors that give rise to nonvanishing structure factors of the $KMgF_3$ lattice. The agreement between the form factors computed from the Gaussian-basis wave functions and those from the numerical wave functions is within 0.2%.

For the valence-band (VB) states, one can achieve high accuracy by including as basis functions the minimal set (Bloch sums of the K $1s,2s,2p,3s,3p$; Mg $1s,2s,2p$; F $1s,2s,2p$ atomic orbitals) plus a number of Bloch sums formed by single Gaussian orbitals (SGO), i.e., using simply $\exp(-\beta r^2)$ or $x\exp(-\beta r^2)$, etc., for the ϕ functions in Eqs. (1). The use of SGO for band-structure calculations has been discussed by Simmons *et al.*[8] The short-range SGO are not used to supplement the minimal set because the former control only the part of the electron cloud near the nuclei which remains free-ion-like. As to the long-range SGO, it has been shown[4] that two single-Gaussian Bloch sums (normalized) formed by long-range SGO of different β are nearly identical even though the two individual Gaussians are quite distinct. For instance we find that single-Gaussian Bloch sums with $\beta<0.1$ merely duplicate the $\beta=0.1$ one in the present work. The Bloch sums of the middle-range SGO are most effective in strengthening the variation freedom of the basis set. Guided by test calculations using various combinations of SGO, we select the following set of single-Gaussian supplement: three s type ($\beta=0.977\,055$, 0.396 147, 0.10) and three p type ($\beta=1.731\,93$, 0.620 64, 0.10) SGO for Mg, two s type ($\beta=0.620\,64$, 0.10) and two p type ($\beta=0.620\,64$, 0.206 990) for K, and three s type ($\beta=0.977\,055$, 0.396 147, 0.10) and three p type ($\beta=0.977\,055$, 0.620 64, 0.206 990) for F. This makes a set of 85 Bloch-sum functions. Since the crystal charge density is dictated entirely by the wave functions of the occupied states, this basis set should be sufficient for determining the SCF crystal potential.

As a starting point for an SCF energy-band calculation, we take the zeroth-order approximation of the crystal electron density as a superposition of the free-atom electron density of the K^+, Mg^{2+}, and F^- ions at the appropriate sites,

$$\rho^{(0)}_{\rm cry}(\vec{r})=\sum_\nu\sum_{i=1}^{3}[\rho_{Mg^{2+}}(\vec{r}-\vec{R}_\nu)+\rho_{F^-}(\vec{r}-\vec{R}_\nu-\vec{t}_i)+\rho_{K^+}(\vec{r}-\vec{R}_\nu-\vec{t}\,')]\,.\tag{4}$$

This gives directly the zeroth-order crystal Coulomb potential $V_C^{(0)}$. For the exchange interaction we use the

standard $X\alpha$ approximation,[9]

$$V_X=-(\tfrac{3}{2})\alpha[3\rho_{\rm cry}(\vec{r})/\pi]^{1/3} . \tag{5}$$

We first choose $\alpha=1$ for the exchange parameter. (In Sec. IV we vary the exchange parameters and study their effects on the energy bands.) To handle this term, we compute the values of $[\rho^{(0)}_{\rm cry}(\vec{r})]^{1/3}$ for 353 nonequivalent points in a unit cell, and least-squares fit them to a lattice superposition of certain localized functions,

$$[\rho^{(0)}_{\rm cry}(\vec{r})]^{1/3}=\sum_{\nu}\sum_{i=1}^{3}[g_{2c}(\vec{r}-\vec{R}_\nu)+g_a(\vec{r}-\vec{R}_\nu-t_i)+g_{1c}(\vec{r}-\vec{R}_\nu-\vec{t}\,')] , \tag{6}$$

where the subscripts $1c$, $2c$, and a stand for monovalent cation, divalent cation, and anion, respectively. We find it possible to obtain a very good fit by taking all the g functions as being spherically symmetrical and of the form[10]

$$\sum_i a_i\exp(-\zeta_i r)+\sum_j a'_j r^2\exp(-\xi_i r) . \tag{7}$$

The crystal potential (including both the Coulomb and exchange part) is expanded in a Fourier series

$$V_{\rm cry}(\vec{r})=\sum_\nu V(\vec{K}_\nu)\cos\vec{K}_\nu\cdot\vec{r} , \tag{8}$$

where $\vec{K}_\nu$ designates a reciprocal-lattice vector of the sc system, and $V(\vec{K}_\nu)$ can be determined from $\rho_{Mg^{2+}}(\vec{r})$, $\rho_{F^-}(\vec{r})$, $\rho_{K^+}(\vec{r})$, $g_{2c}(\vec{r})$, $g_a(\vec{r})$, and $g_{1c}(\vec{r})$ in a manner similar to Eq. (6) of Ref. 11. This approximate version of the crystal potential may be referred to as the overlapping-atomic-charge (OAC) model. It differs from the overlapping-atomic-potential (OAP) model in that the OAP model further approximates the exchange potential as the sum of the $\rho^{1/3}$ of the individual atoms rather than the cubic root of the sum of the atomic charge density. The OAC model generally provides a better approximation than does OAP because the latter tends to overestimate the exchange term in the region where charge density is small.

With the OAC crystal potential and the basis set mentioned earlier, we compute the overlap and Hamiltonian matrix elements by the Gaussian technique which has been described in the literature.[3,4] Upon solving the secular equations for four $\vec{k}$ points in the Brillouin zone (BZ), i.e., Γ, X, M, and R (see Fig. 1), we obtain the first-order crystal electron density from the occupied-state wave functions through a four-point numerical integration over the BZ. We compute the electron density and its cubic root for 353 points within a fundamental wedge of a unit cell, and perform a local decomposition by least-squares fit,

$$\rho^{(1)}_{\rm cry}(\vec{r})=\sum_{\nu}\sum_{i=1}^{3}[\rho^{(1)}_{2c}(\vec{r}-\vec{R}_\nu)+\rho^{(1)}_a(\vec{r}-\vec{R}_\nu-\vec{t}_i)+\rho^{(1)}_{1c}(\vec{r}-\vec{R}_\nu-\vec{t}\,')] , \tag{9}$$

$$[\rho^{(1)}_{\rm cry}(\vec{r})]^{1/3}=\sum_{\nu}\sum_{i=1}^{3}[g^{(1)}_{2c}(\vec{r}-\vec{R}_\nu)+g^{(1)}_a(\vec{r}-\vec{R}_\nu-\vec{t}_i)+g^{(1)}_{1c}(\vec{r}-\vec{R}_\nu-\vec{t}\,')] , \tag{10}$$

where the superscript (1) designates first iteration and the functions $\rho_i(\vec{r})$ and $g_i(\vec{r})$ may be expanded by spherical harmonics as

$$\sum_l f_l(r)\sum_m C_l^m Y_{lm}(\theta\phi) .$$

Each $f_l(r)$ is in the exponential form of Eq. (7). When the charge density is written in terms of $\exp(-\xi r)$, the expression for the Coulomb potential can be integrated analytically. [Evaluation of the Coulomb potential would be more complicated if one used Gaussians to fit $f_l(r)$.]

The local cubic symmetry around the K and Mg sites excludes the $l=1,2,3$ terms for the cations, whereas the anion local tetragonal symmetry excludes the $l=1$ and $l=3$ terms for F^-. We are able to fit $\rho^{(1)}_{\rm cry}(r)$ and its cube root accurately using only $l=0$ terms. This does not mean that the crystal charge density around each site is spherical. For instance the crystal charge around a Mg site consists of the spherical term $\rho_{2c}(r)$ plus contribution from the F^- terms $\rho_a(\vec{r}-\vec{R}_\nu-\vec{t}_i)$ situated at the six first-nearest-neighbor sites and the K^+ terms $\rho_{1c}(\vec{r}-\vec{R}_\nu-\vec{t}\,')$ at the eight second-nearest

neighbor sites, etc. The contribution from the neighboring ions produces a nonspherical component of $\rho_{cry}(\vec{r})$ around the Mg site. Nevertheless as a test calculation we include the $l>0$ terms in the curve fit and find that the only appreciable $l>0$ component is the $l=2$ term of F^-. Inclusion of this term decreases the band gap by 0.03 eV and has negligible effects on the x-ray structure factors except a change of 0.15 in the (100) value and 0.09 in the (110) value. A more detailed account of the x-ray structure factors is given in Sec. III B.

From $\rho^{(1)}$ and $g^{(1)}$ we derive the Fourier coefficients of the improved crystal potential which produces a set of improved energies and wave functions. The iteration procedure is repeated to arrive at an SCF solution. Computational methods for the SCF iteration have been described.[11–13]

For calculating conduction-band (CB) energies we employ an extended basis set of 124 functions which cover Bloch sums of occupied orbitals, unoccupied orbitals, and SGO. They include Mg $1s,2s,3s,2p,3p,3d$ orbitals, K $1s,2s,3s,4s,2p,3p,4p,3d$ orbitals, F $1s,2s,3s,2p,3p,3d$ orbitals, two s type and two p type ($\beta=0.62064$, 0.206990) SGO for all three kinds of atoms, and two d type ($\beta=0.620640$, 0.396147) SGO for K. Figure 2 shows the SCF energy bands calculated with this extended basis set and $\alpha=1$. The energy of the upper Γ_{15} state of the VB is set to zero. A sketch of the BZ for sc crystals is included in Fig. 1. We arrive at the 124-function set by starting with a

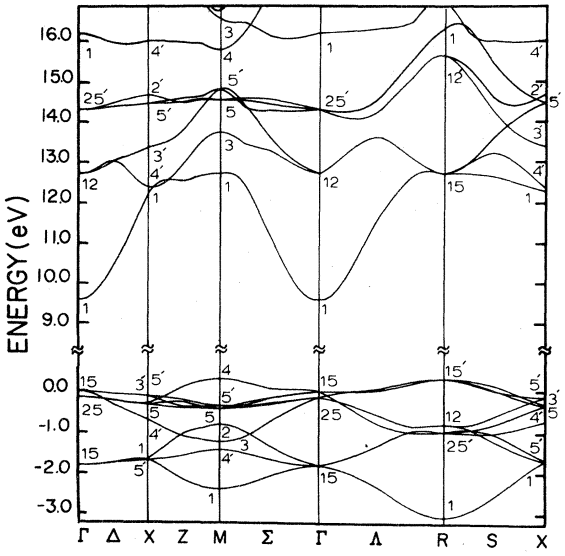

FIG. 2. Valence and conduction bands of $KMgF_3$ calculated by using exchange parameters $\alpha=1$, $\beta=0$.

large set of 209 functions which include additional s-, p-, and d-type single-Gaussian Bloch sums for K, Mg, and F. The calculated CB energies at the Γ, X, M, and R points are monitored as the various single-Gaussian basis functions are removed. The energies of the lower CB (below 20 eV) at Γ, X, M, and R derived from the 124-function set and from the 209-function set differ by no more than 0.3 eV. Band energies for four high-symmetry

TABLE I. SCF electronic energies of the $KMgF_3$ crystal (with exchange parameter $\alpha=1$, $\beta=0$) in units of eV. The subscripts v and c represent VB and CB, respectively.

	Energies		Energies		Energies
Γ_{15v}	−1.82	X'_{3c}	13.36	M'_{5c}	14.79
Γ_{25v}	−0.15	X'_{5c}	14.45	M_{4c}	15.77
Γ_{15v}	0.0	X'_{2c}	14.66	M_{3c}	16.52
Γ_{1c}	9.60	X'_{4c}	15.98	M_{1c}	16.72
Γ_{12c}	12.69	X_{1c}	17.98	M'_{4c}	18.49
Γ'_{25c}	14.29	X_{5c}	19.33	R_{1v}	−3.09
Γ_{1c}	16.15	M_{1v}	−2.42	R'_{25v}	−0.99
Γ_{15c}	18.62	M'_{4v}	−1.44	R_{12v}	−0.80
X'_{5v}	−1.69	M_{3v}	−1.25	R'_{15v}	0.32
X_{1v}	−1.65	M_{2v}	−0.81	R_{15c}	12.69
X'_{4v}	−0.71	M_{5v}	−0.43	R'_{12c}	15.61
X_{5v}	−0.33	M'_{5v}	−0.36	R_{1c}	16.24
X'_{3v}	−0.29	M_{4v}	0.31	R'_{2c}	16.92
X_{5v}	−0.12	M_{1c}	12.71	R'_{25c}	17.48
X_{1c}	12.27	M_{3c}	13.73	R_{15c}	18.74
X'_{4c}	12.37	M_{5c}	14.54		

points in the BZ are given in Table I. The crystal charge density calculated from these extended-basis VB wave functions (which allow for d-orbital admixture) differs very little from the results based on the smaller set (85 functions) used earlier. When the extended-basis charge density is decomposed as in Eqs. (9) and (10), the only appreciable anisotropy component of ρ_i and g_i is again the $l=2$ term of F^-. Comparing the x-ray structure factors derived from the two basis sets, we find a difference of only 0.09 for (100) and less than 0.04 for the others.

III. RESULTS

A. Valence band

The VB wave functions are dominated by the F $2p$ orbitals. Since there are three F atoms per unit cell, one finds three sets of triply degenerate states at the Γ point. The bottom of the VB is at R. The wave function for the R_1 state consists of F $2p$ orbitals perpendicular to each face of the cube. The positive loops of all six orbitals associated with one cube all point toward its center whereas those associated with the next cube point away from its center. The strong overlap of the F orbitals at the center of each cube lowers the energy of the R_1 state. The density of states (DOS) of the VB is calculated by using the linear, analytic tetrahedron method[14] and shown in Fig. 3. The leading peak occurs at an energy close to the Γ_{25} and the upper Γ_{15} states, and is a result of the flat bands near that energy. The width of the VB is 3.3 eV.

B. X-ray structure factors

To calculate the x-ray structure factors, we decompose the SCF crystal electron density into a

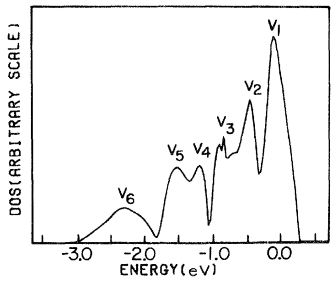

FIG. 3. Density of states of the valence bands of $KMgF_3$ calculated by using exchange parameters $\alpha=1$, $\beta=0$.

lattice superposition similar to Eq. (9), i.e.,

$$\rho_{\rm cry}^{\rm SCF}(r)=\sum_{\nu}\sum_{i=1}^{3}[\rho_{2c}^{S}(\vec{r}-\vec{R}_\nu)+\rho_a^S(\vec{r}-\vec{R}_\nu-\vec{t}_i)+\rho_{1c}^S(\vec{r}-\vec{R}_\nu-\vec{t}')] . \quad (11)$$

From the $\rho^S(r)$ functions we determine the structure factors $F(hkl)$ for the reciprocal-lattice vector characterized by (hkl). We apply the B factors for temperature correction using the parameters given by Chelkowski *et al.*,[15] and also correct for anomalous dispersion.[16] As shown in Table II, the calculated structure factors differ significantly from the experimental values of Chelkowski *et al.*,[15] especially for the [200] and [220]. Up to this point we use only $\alpha=1$ for the exchange parameter. Since $\alpha=\frac{2}{3}$ is believed to give a better description of the ground state, we have repeated the SCF band calculation with $\alpha=\frac{2}{3}$. This leads to a second set of calculated structure factors which are included in Table II. A third set is generated by using the Hartree-Fock free-ion charge densities. As seen in Table II the second and third sets are very similar to each other but do not agree well with the experimental values of Ref. 15. To pursue this point we try to reproduce the calculated $F_c(hkl)$ of Ref. 15 by using their formula for $F_c(hkl)$, their B factors, and the free-ion form factors from the International Table,[17] but no dispersion correction. The resulting values differ substantially from those of Ref. 15. In fact if we leave out the B-factor correction, then we can quite well duplicate the $F_c(hkl)$ values (calculated) of Ref. 15.

For absolute calibration the experimental structure factors (relative) are fitted to the calculated values with the B factors and a multiplicative normalization constant as adjustable parameters. Thus, we feel that the absolute experimental structure factors given in Ref. 15 should be reexamined. To this end we "recalibrate" the experimental data of Ref. 15 by fitting them to our three sets of calculated structural factors mentioned earlier with adjustable B factors and normalization constant. Even allowing a wide range the B factors, we are unable to get a fit with an average percentage difference, the R factor defined in Ref. 15, below 12%. This is a very large discrepancy compared to the corresponding R factors of 0.8% for LiF,[18] 1% for CaF_2,[19] and 0.9% for Si.[20] As will be dis-

TABLE II. Comparison of experimental x-ray structure factors with three sets of theoretical values (with temperature and dispersion corrections) based on (i) SCF band calculating with $\alpha=1$, (ii) SCF band calculation with $\alpha=\frac{2}{3}$, and (iii) a free-ion charge superposition.

	Expt.	Theoretical $F(hkl)$		
hkl	$F(hkl)$	$\alpha=1$	$\alpha=\frac{2}{3}$	Free-ion
100	−2.60	−2.34	−2.28	−2.37
110	15.3	16.06	15.97	16.09
111	24.9	24.85	23.90	23.93
200	49.2	38.41	37.16	37.29
210	−3.2	−2.40	−2.24	−2.29
211	12.2	12.76	12.70	12.72
220	24.7	28.72	27.69	27.74
221	0.0	−2.02	−1.83	−1.86
300	0.0	−2.02	−1.83	−1.86
310	11.9	10.69	10.61	10.64
222	22.4	23.08	22.31	22.28
321	10.0	9.24	9.17	9.19
400	19.1	19.36	18.79	18.73
411	8.7	8.12	8.04	8.08
300	8.7	8.13	8.07	8.08

cussed more fully in Sec. IV, we have recalculated the band structure using three other versions of the exchange-correlation potential, yet the resulting theoretical structure factors do not align any better with the data of Ref. 15. The divergence of many of the experimental structure factors from the theoretical values based on free-ion superposition and on several sets of band structures suggests that serious experimental difficulties exist and further clarification is needed before making a meanful comparison.

C. Conduction bands

The CB structure and DOS are shown in Figs. 2 and 4, respectively. The bottom of the CB is a Γ_1 state which is composed of s orbitals of all three kinds of atoms. A few eV above the CB edge are the Γ_{12} and Γ'_{25} states which are predominantly K $3d$ states with only little Mg $3d$ admixture. This is in line with the atomic picture since in the free atoms the $3d$ state of Mg^+ is 8.7 eV above the ground state whereas the $3d$ state of K is only 2.7 eV above $4s$.[21] There is no mixing with the s and p orbitals of the F atoms on account of symmetry. A large part of the bands connected to Γ_{12} and Γ'_{25} is quite flat. We will refer to these bands as the K $3d$ bands. They predominate in the energy range of 3—5.5 eV above the onset of the CB, and are responsible for the two peaks labeled as C_2 and C_3 in the DOS (Fig. 4). This is similar to the case of CaF_2 in which the bottom of the CB is s-like with the Ca $3d$ bands 2.3—3.5 eV above it and the DOS of the Ca $3d$ bands overshadows those of the bands immediately above and below them (s and p type).[22] Peak C_4 in Fig. 4 is due to part of a band which is rather undispersive. As will be seen in Sec. IV, this peak disappears if we set the exchange parameter α to 1.33. Thus, the formation of peak C_4 appears not to be related to fundamental properties of the crystal.

The calculated direct bandgap at Γ is 9.6 eV. Takahashi and Onaka[23] reported ultraviolet-reflection measurements and an optical dielectric

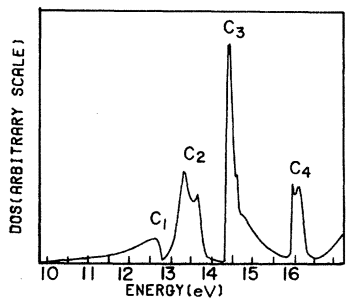

FIG. 4. Density of states of the conduction bands of $KMgF_3$ calculated by using exchange parameters $\alpha=1$, $\beta=0$.

function (ϵ_2) but did not deduce a value for the bandgap *per se* from their data. Reflection spectra for $KMgF_3$ have also been measured by Beaumont *et al.*,[24] and their results are similar to those of Ref. 23. The dielectric function ϵ_2 given by Takahashi and Onaka shows a sharp peak at 11.9 eV, which is identified as an exciton transition. If we take the rise of ϵ_2 following the exciton peak as the onset of band-to-band transition, the Γ bandgap is estimated to be 12.4 eV. However, Takahashi and Onaka interpret some of the structure immediately after the 11.9-eV peak as being excitons of $n=2,3,\ldots$. This interpretation would place the bandgap slightly above 12.4 eV. In any case it is clear that our calculated band gap of 9.6 eV is too small.

D. Joint density of states

The joint density of states (JDOS) between the VB and CB is given in Fig. 5. The structures in the range of 13.3—15.1 eV can be traced to transitions from the upper part of VB to the K 3*d* CB states. This can be seen by referring to the DOS peaks labeled as V_1, V_2, V_3, V_4, V_5, and V_6 for the VB in Fig. 3, and the peaks C_1, C_2, C_3, and C_4 for the CB in Fig. 4. The $V_1 \rightarrow C_2$, $V_1 \rightarrow C_3$, and $V_2 \rightarrow C_3$ energy increments are, respectively, 13.4, 14.5, and 14.9 eV, corresponding closely to the energies of peaks I, II, and III of the JDOS in Fig. 5. The small structure of the JDOS at 14.2 eV may be attributed to $V_3 \rightarrow C_2$. Between 15.5 and 16.5 eV, the structures of the JDOS may be associated with $V_4 \rightarrow C_3$ (15.6 eV), $V_5 \rightarrow C_3$ (16.0 eV), and $V_1 \rightarrow C_4$ (16.1 eV). For comparison we present as a dashed curve in Fig. 5 the experimental dielectric function of Takahashi and Onaka[22] (the leading exciton peak of ϵ_2 at 11.9 eV is not included since there is no counterpart in the JDOS). We see a remarkable resemblance in the two curves. Takahashi and Onaka[23] assign the shoulder "*a*" of their data (shown as a dashed curve in Fig. 5 of this paper) as a superposition of $n=2,3,\ldots$ exciton bands extending continuously to band-to-band transitions. Thus, at least part of the observed structure of ϵ_2 at 13—14 eV may be attributed to band-to-band transitions. If we were to make the energy-band model of Figs. 2—4 and the experimental data consistent with each other, part of the 13—14 eV structure in ϵ_2 should be assigned to transitions from the top of the VB to the lower part of the K 3*d* CB. The calculated band gap, however, is considerably smaller than the experimental value as is evident in Fig. 5. Thus, it appears that in our band diagram (Fig. 2), the K 3*d* bands are in the correct energy range but the bottom of the CB is too low. To make our band structure compatible with the experimental data, we would have to move the bottom of the CB (Γ_1) upward so that it is only about 1 eV below the Γ_{12} state. This is, of course, only a speculation. An important question is whether with an improved calculation one can obtain a band structure which gives a correct band gap and also accounts quantitatively for the observed structures in the optical data. This point will be studied in the following section.

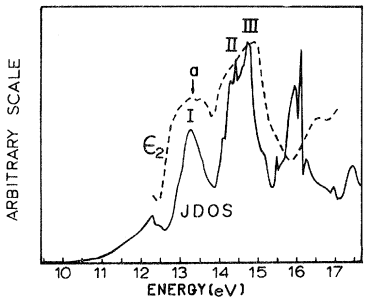

FIG. 5. Solid curve is the joint density of states between the valence bands and conduction bands of $KMgF_3$ calculated by using exchange parameters $\alpha=1$, $\beta=0$. The dashed curve is the measured dielectric function (imaginary part) reported in Ref. 15.

IV. $X\alpha$ AND $X\alpha\beta$ EXCHANGE POTENTIALS

Recent SCF energy-band studies indicate that with the full Slater exchange potential ($\alpha=1$) the calculated band gaps for several strongly ionic crystals, i.e., LiF,[11] LiCl,[25] CaO,[12] CaF_2,[22] and MgO,[26] are 10—20% smaller than the experimental values. For $KMgF_3$ the use of $\alpha=1$ also gives too small a band gap (9.6 eV vs $\sim$12.4 from experiment). We also did an SCF band calculation with $\alpha=\frac{2}{3}$ (Sec. III B) and obtained a 7.2 eV gap. This difficulty may be attributed to the fact that the exchange approximation employed in this work was derived for a free-electron gas, and may not be suitable for ionic crystals with atomic-like charge densities. Particularly the self-interaction term in the Coulomb potential is not fully compensated by the local exchange approximation. Considerable efforts have been directed to treat the self-interaction correction.[27] These techniques have been tested for atoms but application to band-

structure calculations has not been published. As an alternative to the self-interaction-correction approach, we explore in this work the use of other forms of the exchange-correlation potential for an improved description of the band gap and optical properties. One important criterion for the choice of exchange potential is that it can be incorporated into our present computational scheme for SCF energy-band structure without extensive modification.

An obvious, simple way to alter the exchange potential is to let α exceed unity. Upon choosing $\alpha=1.33$, our SCF-LCAO calculation gives a band gap of 12.4 eV for $KMgF_3$. Nevertheless, this procedure is not entirely satisfactory since α is generally assumed to be within the range of 1 and $\frac{2}{3}$.

An interpolation formula for the exchange-correlation potential due to Wigner,[28]

$$V_{\rm xc}(\vec{r})=-[\rho(\vec{r})]^{1/3}\left[0.984+\frac{0.944+8.77[\rho(\vec{r})]^{1/3}}{\{1+12.57[\rho(\vec{r})]^{1/3}\}^2}\right], \tag{12}$$

has been often used. One can regard this formula as having an α which depends on ρ; it is equivalent $\alpha=0.67$ for large ρ and to $\alpha=1.30$ for small ρ with a smooth transition between the two regions. With this exchange-correlation potential, our SCF-LCAO calculation gives a band gap of 7.1 eV which is very close to the result of $\alpha=\frac{2}{3}$ but too small for the interpolation formula to be useful for the study of CB states.

Herman, Van Dyke, and Ortenburger[29] have suggested an improved version of the statistical exchange approximation by including an inhomogeneity correction term,

$$V_{X\alpha\beta}=-[\alpha+\beta G(\rho)]\tfrac{3}{2}(3\rho/\pi)^{1/3}, \tag{13}$$

$$G(\rho)=\rho^{-2/3}[(\tfrac{4}{3})(\nabla\rho/\rho)^2-2\nabla^2\rho/\rho]. \tag{14}$$

The new exchange potential introduces another parameter β (not to be confused with the Gaussian exponents β in Sec. II), hence is known as the $X\alpha\beta$ method. At certain points in the crystal, $\beta G(\rho)$ may become so negative that it overpowers the α term. To avoid this complication, an alternative form

$$V_{X\alpha\beta}=-\alpha\{1+\tanh[\beta G(\rho)/\alpha]\}\tfrac{3}{2}(3\rho/\pi)^{1/3}, \tag{15}$$

has been proposed.[30] Since $\tanh x$ approaches x and -1, respectively, for $x\to 0$ and $x\to\infty$, Eq. (15) is close to Eq. (13) for $\beta G(\rho)/\alpha$ below 1, but remains negative even at very large value of $G(\rho)$. Herman[31] has suggested an alternative version of Eq. (15),

$$V_{X\alpha\beta}=-[\alpha+\beta\tanh G(\rho)]\tfrac{3}{2}(3\rho/\pi)^{1/3}. \tag{16}$$

In the part of the crystal where the charge density is atomiclike, $G(\rho)$ is large and positive so that $\tanh G(\rho)$ is close to 1. In the interatomic region $G(\rho)$ turns highly negative with $\tanh G(\rho)$ approaching -1. Compared to the simple $X\alpha$ exchange, this $X\alpha\beta$ exchange (for $\beta>0$) deepens the potential well near the atoms, and weakens it in the space between atoms. Since the VB states are atomiclike and the CB wave functions are more diffuse, the $X\alpha\beta$ term in Eq. (16) has the desired effect of lowering the VB and lifting the CB for positive values of β. Analyses of the gradient term by a more fundamental approach have appeared in the literature.[32] However, in our work we will choose β empirically so as to improve the band gap while keeping α within the conventional range. Choosing $\alpha=1$ and $\beta=\frac{1}{6}$, we obtain an SCF band gap of 12.4 eV.[33] If we use a smaller value of α, then a larger β would be needed to keep the band gap at 12.4 eV. Since the β term is presumably a correction to the α term, it is not desirable to have β much larger than $\frac{1}{6}$. While rigorous theoretical

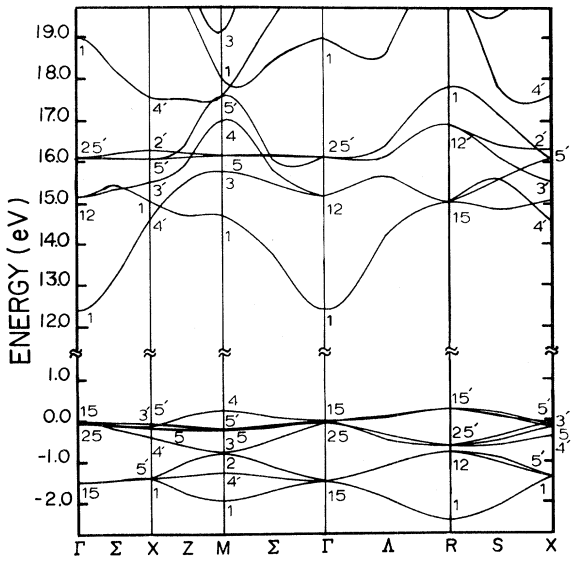

FIG. 6. Valence and conduction bands of $KMgF_3$ calculated by using exchange parameters $\alpha=1.33$, $\beta=0$.

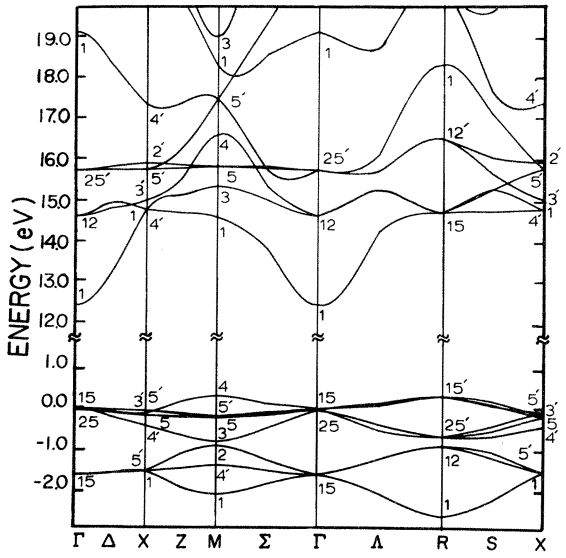

FIG. 7. Valence and conduction bands of $KMgF_3$ calculated by using exchange parameters $\alpha=1$, $\beta=\frac{1}{6}$.

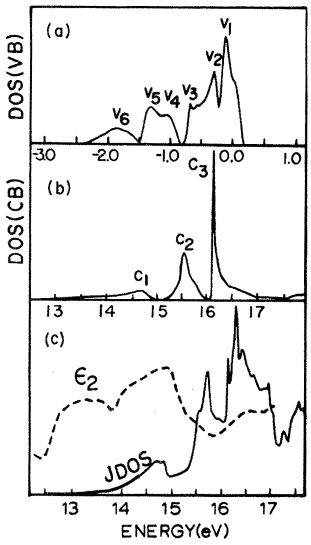

FIG. 8. (a) Density of states of the valence bands, (b) density of states of the conduction bands, and (c) joint density of states between the valence bands and conduction bands calculated by using exchange paremeters $\alpha=1.33$, $\beta=0$. The dashed curve in (c) is the measured dielectric function (imaginary part) reported in Ref. 15.

justifications for our selection of the exchange parameters are lacking, the $X\alpha\beta$ scheme does provide us with a band gap close to the experimental value so that we can compare the $X\alpha\beta$ band structure with the $X\alpha$ calculations and with the optical data.

The $X\alpha$ exchange may be regarded as a special case of the $X\alpha\beta$ method with $\beta=0$. The results described in Sec. III correspond to $\alpha=1$, $\beta=0$, abbreviated as ($\alpha\beta$:1,0). We present in Figs. 6 and 7 two additional SCF band structures, one obtained by using $\alpha=1.33$, $\beta=0$ [denoted by ($\alpha\beta$:1.33,0)], and the other using $\alpha=1$, $\beta=\frac{1}{6}$ [denoted by ($\alpha\beta$:1,$\frac{1}{6}$)]. These two sets of new energy bands have a 12.4 eV band gap which is much larger than the 9.6 eV of the ($\alpha\beta$:1,0) case. For comparing the three different band structures, the DOS (VB and CB) and JDOS of the ($\alpha\beta$:1.33,0) and ($\alpha\beta$:1,$\frac{1}{6}$) results are shown in Figs. 8 and 9. The general features of the VB are alike for all three cases. The VB width is 2.6 eV for ($\alpha\beta$:1.33,0), 2.8 eV for ($\alpha\beta$:1,$\frac{1}{6}$), and 3.3 eV for ($\alpha\beta$:1,0). These values are appreciably smaller than 4.1 and 4.0 eV from ($\alpha\beta$:$\frac{2}{3}$,0) and the interpolation formula, respectively. In Table III the structure factors for the five exchange models used in this study are presented along with those obtained by free-ion superposition. Here, no temperature or dispersion correction is applied. These structure factors are intended as a description of the crystal charge density rather than for comparison with experiment. The ($\alpha\beta$:1.33,0) and ($\alpha\beta$:1,$\frac{1}{6}$) sets in Table III are very close to each other and exhibit a slightly larger difference from the structure factors of ($\alpha\beta$:1,0). The agreement between the results of the free-ion model and ($\alpha\beta$:$\frac{2}{3}$,0) is very good, and is consistent with previous studies of ionic crystals: LiF and LiCl.[18,34] In particular it is interesting to note the linearity between the results of the three $X\alpha$ potentials. Thus, it may be difficult to pick the best choice of α from the experimental structure factors because of the normalization procedure. Also the differences between the results of ($\alpha\beta$:$\frac{2}{3}$,0) and the interpolation formula are surprisingly small.

One finds larger variations in the CB with respect to the exchange parameters. The energy spacing between the Γ_{12} conduction state and the onset of the CB varies appreciably: 3.1 eV for ($\alpha\beta$:1,0), 2.7 eV for ($\alpha\beta$:1.33,0), and 2.2 eV for ($\alpha\beta$:1,$\frac{1}{6}$). For both the ($\alpha\beta$:1.33,0) and ($\alpha\beta$:1,$\frac{1}{6}$) calculations, we find two prominent peaks (C_2 and C_3) associated with the K 3d states in the DOS of the CB [Figs. 8(b) and 9(b)], but no structure corresponding to peak C_4 in Fig. 4. The ($\alpha\beta$:$\frac{2}{3}$,0) form and the interpolation formula give an unrealistically low band gap, thus these two exchange models will not be considered for our discussion of

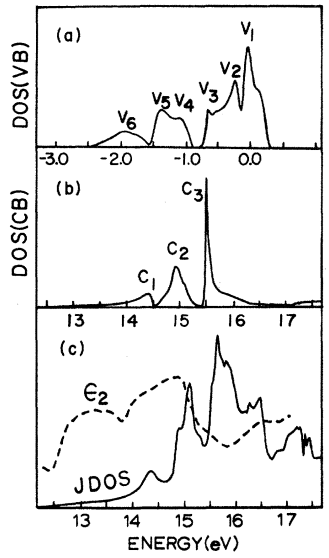

FIG. 9. (a) Density of states of the valence bands, (b) density of states of the conduction bands, and (c) joint density of states between the valence bands and conduction bands calculated by using exchange parameters $\alpha=1$, $\beta=\frac{1}{6}$. The dashed curve in (c) is the measured dielectric function (imaginary part) reported in Ref. 15.

optical properties.

In the energy range of 15—17 eV, the JDOS for the two new band structures in Figs. 8(c) and 9(c) are dominated by transitions from the VB to the K $3d$ bands. The energies of the JDOS peaks match well with the energy increments between the appropriate DOS peaks, i.e., V_1 and V_2 of the VB [Figs. 8(a) and 9(a)] to C_2 and C_3 of the CB [Figs. 8(b) and 9(b)]. However, the major structures of the JDOS from both ($\alpha\beta$:1.33,0) and ($\alpha\beta$:1,$\frac{1}{6}$) calculations occur at higher energies than those of the experimental dielectric function[23] which is also included in Figs. 8(c) and 9(c). Even if we attribute the entire broad peak of ϵ_2 at 13—14 eV to excitons and exclude it from band-to-band consideration, the agreement between theory and experiment is not entirely satisfactory on a quantitative scale.

V. DISCUSSION AND SUMMARY

We have calculated SCF energy-band structures for the $KMgF_3$ crystal under the Hartree-Fock-Slater scheme. To ensure good accuracy for the VB and the lower CB, we employ a basis set of

TABLE III. Theoretical x-ray structure factors (without temperature and dispersion corrections) calculated by using five different versions of exchange approximation: interpolation formula, $\alpha=\frac{2}{3}$, $\alpha=1$, $\alpha=1.33$, and ($\alpha\beta$:1,$\frac{1}{6}$). Included are also the values obtained by free-ion charge superposition.

		Theoretical $F(hkl)$				
hkl	Interp.	$\alpha=\frac{2}{3}$	$\alpha=1$	$\alpha=1.33$	($\alpha\beta$:1,$\frac{1}{6}$)	Free-ion
100	−1.88	−1.86	−1.92	−1.95	−2.07	−1.95
110	15.92	15.94	16.01	16.11	16.00	16.05
111	24.38	24.32	25.31	26.40	26.09	24.36
200	38.05	37.98	39.27	40.65	40.23	38.11
210	−1.67	−1.65	−1.84	−2.00	−2.01	−1.72
211	13.21	13.22	13.29	13.45	13.37	13.24
220	29.34	29.28	30.39	31.67	31.20	29.34
221	−1.07	−1.05	−1.29	−1.53	−1.49	−1.09
300	−1.07	−1.05	−1.29	−1.53	−1.49	−1.09
310	11.53	11.54	11.64	11.78	11.74	11.56
311	13.56	13.52	14.08	14.77	14.42	13.45
222	24.50	24.45	25.32	26.36	25.91	24.43
320	−0.42	−0.40	−0.66	−0.94	−0.84	−0.42
321	10.42	10.43	10.52	10.66	10.65	10.44
400	21.41	21.38	22.04	22.87	22.50	21.31
322	0.14	0.16	−0.09	−0.39	−0.25	0.16
410	0.17	0.18	−0.10	−0.39	−0.26	0.16
330	9.62	9.62	9.69	9.83	9.83	9.63
411	9.58	9.58	9.67	9.82	9.82	9.63

124 functions consisting of Bloch sums of atomic orbitals and of single Gaussians. The VB wave functions are composed predominantly of F $2p$ orbitals. The bottom of the CB is an s-like Γ_1 level. Slightly above it is a group of states which may be characterized as K $3d$ bands with high DOS. Transitions from the VB to the K $3d$ bands are responsible for the optical dielectric function in the energy range involved.

The calculated JDOS using $\alpha=1$ for the exchange parameter agrees with the experimental dielectric functions in the range of 13—16 eV, but the calculated band gap is too low. For highly ionic crystals the SCF band gap using $\alpha=1$ is generally smaller than the experimental value. In this paper we study five different versions of the local exchange approximation: the $X\alpha$ potential with three different values of $\alpha(1, \frac{2}{3}, 1.33)$, the interpolation formula, and the $X\alpha\beta$ potential. The $\alpha=\frac{2}{3}$ version and the interpolation formula yield even smaller band gap than does $\alpha=1$. By setting α to 1.33 or by using the $X\alpha\beta$ method with β chosen empirically, we obtain an SCF band gap consistent with the optical experiment. However, the JDOS derived from these two new band models deviate appreciably from the experimental ϵ_2, and agreement is seen only on a qualitative level. On the other hand the VB is less sensitive to the choice of α and β, except for a minor narrowing of the VB width as compared to the $(\alpha\beta{:}1,0)$ calculation, which in turn, gives a smaller VB width than does $(\alpha\beta{:}\frac{2}{3},0)$.

The problem of underestimation of band gap for highly ionic crystals by Hartree-Fock-Slater calculation is a fundamental one. In this paper we seek improvement through the $X\alpha$ (with $\alpha>1$) and $X\alpha\beta$ procedures with only a limited degree of success. Nevertheless, these methods may be used, in the absence of a more appropriate exchange potential, to provide a band structure with a reasonable description of the VB and a band gap close to the experimental value. An improvement of the exchange approximation based on a more fundamental approach such as the self-interaction correction is needed.

ACKNOWLEDGMENTS

We wish to thank Dr. F. Herman for suggesting the $X\alpha\beta$ potential given in Eq. (16) and stimulating discussions. This research was supported by the National Science Foundation.

[1]L. F. Mattheiss, Phys. Rev. B 6, 4718 (1972).
[2]A. H. Kahn and A. J. Leyendecker, Phys. Rev. 135, A1321 (1964).
[3]R. C. Chaney, T. K. Tung, C. C. Lin, and E. E. Lafon, J. Chem. Phys. 52, 361 (1970); E. E. Lafon and C. C. Lin, Phys. Rev. 152, 579 (1966).
[4]E. E. Lafon, R. C. Chaney, and C. C. Lin, in *Computational Methods in Band Theory,* edited by P. M. Marcus, J. F. Janak, and A. R. Williams (Plenum, New York, 1971), p. 284.
[5]S. Huzinaga, J. Chem. Phys. 42, 1293 (1965).
[6]A. J. H. Wachters, J. Chem. Phys. 52, 1033 (1970).
[7]F. Herman and S. Skillman, *Atomic Structure Calculations* (Prentice-Hall, Englewood Cliffs, N.J., 1963).
[8]J. E. Simmons, C. C. Lin, D. F. Fouquet, E. E. Lafon, and R. C. Chaney, J. Phys. C 8, 1549 (1975).
[9]J. C. Slater, *The Self-Consistent Field for Molecules and Solids* (McGraw-Hill, New York, 1974).
[10]The exponential parameters in Eq. (7) are chosen in the following manner. We arrive at the set of ξ_i by performing a nonlinear least-squares fit of the free-ion charge densities of K^+, Mg^+, and F^- to the form $\sum_i a_i \exp(-\xi_i r)$. The ξ's are chosen so that all the $r^2\exp(-\xi_i r)$ terms have their peak values at radial distances corresponding more or less to the interstitial region and therefore can reproduce the deviation of the crystal charge density from free-ion superposition.
[11]R. C. Chaney, E. E. Lafon, and C. C. Lin, Phys. Rev. B 4, 2734 (1971).
[12]U. Seth and R. C. Chaney, Phys. Rev. B 12, 5923 (1975).
[13]R. Heaton and E. E. Lafon, Phys. Rev. B 17, 1958 (1978).
[14]J. Rath and A. J. Freeman, Phys. Rev. B 11, 2109 (1975).
[15]A. Chelkowski, P. Jakubowski, D. Kraska, A. Ratuszna, and W. Zapart, Acta Phys. Pol. A 47, 347 (1975).
[16]D. T. Cromer, Acta Crystallogr. 18, 17 (1965).
[17]*International Tables for X-Ray Crystallography III* (Kynoch, Birmingham, England, 1962).
[18]For a comprehensive discussion of the structure factors in LiF, see A. Zunger and A. J. Freeman, Phys. Rev. B 16, 2901 (1977).
[19]S. Togawa, J. Phys. Soc. Jpn. 19, 1696 (1964).
[20]P. J. E. Aldred and M. Hart, Proc. R. Soc. London Ser. A 332, 239 (1973).
[21]C. E. Moore, *Atomic Energy Levels,* Natl. Bur. Stand. (U.S.) Circ. No. 467 (U.S. GPO, Washington, D. C., 1949).
[22]R. A. Heaton and C. C. Lin, Phys. Rev. B 22, 3629 (1980).
[23]H. Takahashi and R. Onaka, J. Phys. Soc. Jpn. 43, 2021 (1977).
[24]J. H. Beaumont, A. J. Bourdillon, and J. Bordas, J.

Phys. C 10, 333 (1977).
[25]J. G. Harrison and C. C. Lin, Phys. Rev. B 23, 3894 (1981).
[26]R. C. Chaney (private communication).
[27]See, for example, R. D. Cowan, Phys. Rev. 163, 54 (1967); I. Lindgren, Int. J. Quantum Chem. Symp. 5, 411 (1971); J. P. Perdew, Chem. Phys. Lett. 64, 127 (1979); A. Zunger, J. P. Perdew, and G. L. Oliver, Solid State Commun. 34, 933 (1980).
[28]E. P. Wigner, Phys. Rev. 46, 1002 (1934); N. D. Lang and W. Kohn, Phys. Rev. B 1, 4555 (1970).
[29]F. Herman, J. P. Van Dyke, and I. B. Ortenburger, Phys. Rev. Lett. 22, 807 (1969).
[30]K. Schwarz and F. Herman, J. Phys. (Paris) C 3, 277 (1972).
[31]F. Herman (private communication).
[32]See, for example, D. J. W. Geldart and M. Rasolt, Phys. Rev. B 13, 1477 (1976).
[33]The $\tanh G(\rho)$ term in Eq. (16) attains its positive maximum value in most of the core region of each atomic site. However, in the core region between principal-quantum-number shells (e.g., the 1*s* shell and the 2*s*-2*p* shell) for the F and Mg sites, $\tanh G(\rho)$ turns negative because of the abrupt change in slope of the core charge density. As a result, the $X\alpha\beta$ potential given in Eq. (16) inherently contained sharp, narrow dips around the core of each atom site. These dips are smoothed over by curve-fitting in our calculation.
[34]R. A. Heaton, J. G. Harrison, and C. C. Lin (unpublished).